J. Environ. Nanotechnol.
Volume 8, No.1(2019) pp. 13 - 24
ISSN (Print): 2279-0748
ISSN (Online): 2319-5541
doi:10.13074/jent.2019.03.191356

Corrosion Inhibition of Copper in Acid Media using Sparfloxacin – Electrochemical Study

P. Thanapackiam[1*], E. P. Subramaniam[2]

[*1,2]*Department of Chemistry, Coimbatore Institute of Technology, Coimbatore, TN, India.*

Received: 18.10.2018 *Accepted: 02.12.2018*

Abstract

The potentiodynamic polarization technique and electrochemical impedance spectroscopy was used to study the inhibition efficiency of sparfloxacin on the corrosion of copper in acid solutions. Sparfloxacin exhibited good inhibition efficiency and the inhibition action was observed to be of mixed type but with more of cathodic nature. Potential of zero charge studies have been carried out to establish the mechanism of adsorption of the inhibitor onto the metal surface. From the temperature dependence of the corrosion rates, the activation energy (Ea) and the thermodynamic parameters such as the adsorption equilibrium constant (K_{ads}), the free energy of adsorption (ΔG_{ads}), ΔS, ΔH were calculated. The free energy of adsorption close to -40 kJmol^{-1} indicates that the adsorption is through electrostatic coulombic attraction and chemisorption. The adsorption of sparfloxacin molecules obeyed Langmuir adsorption isotherm. Synergistic effect of KCl, KBr, and KI was investigated and enhancement in inhibition efficiency was observed on addition of KI due to synergism.

Keywords: *Acid solutions; Copper; EIS; Potentiodynamic polarization; Sparfloxacin.*

1. INTRODUCTION

Copper is an important engineering material and finds applications in electricity, electronics, chemical industry, building construction, ornamental parts, etc. Even though copper is relatively a noble metal, it is susceptible to corrosion in acids. Copper is exposed to corrosive solution often during processing. The most practical methods for the protection against corrosion in acid media is the use of organic inhibitors containing hetero atoms such as N,O,P,S etc, and/or multiple bonds and aromatic rings.

Owing to strict environmental regulations, low inhibitor toxicity is an important requirement for the applied inhibitors. Because of the low toxicity and high efficiency of sparfloxacin, an attempt has been made in the present work, to describe the corrosion inhibition mechanism and efficiency of sparfloxacin for corrosion of copper in 1.0M HNO_3 and 0.5M H_2SO_4 acid solutions at various concentrations and temperatures using techniques such as polarisation, electrochemical impedance spectroscopy, adsorption studies and surface morphological studies. The thermodynamic and activation parameters for the adsorption process were calculated and discussed.

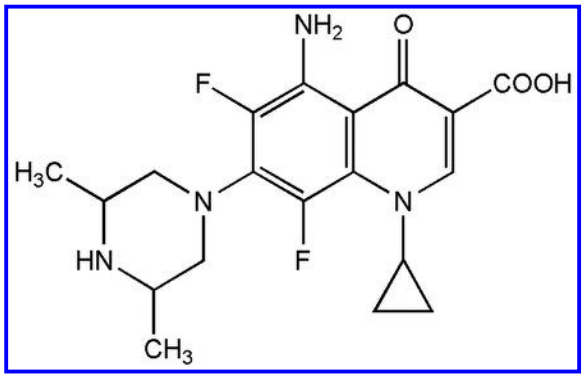

Fig. 1: Structure of sparfloxacin

2. EXPERIMENTS

2.1Materials

Copper specimens having a composition of 99.5 wt. % Cu, 0.116 wt. % Si, 0.019 wt. % Al, 0.003

*** P.Thanapackiam**
e-mail: pthanapackiam@rediffmail.com

wt. % Ni and 0.002 wt.% Mn and dimensions 2.5cm x 1cm x 0.1cm were used for weight-loss measurements.

These specimens were polished successively with emery papers of 1/0, 2/0, 3/0, 4/0 and 5/0 grades, degreased with acetone and dried. A Teflon coated cylindrical copper electrode of exposed area 0.2826 cm^2 having the previously described composition was used for electrochemical studies. Prior to these measurements, the surface was polished to mirror finish, using emery papers of various grades and degreased with acetone and blown dry with nitrogen. All experiments were carried out at room temperature of 301 ± 1 K. All the chemicals were of analytical reagent grade (Sigma Aldrich), E Merck (India) and were used without further purification. Inhibitor stock solutions were prepared in 2.5 M solution of respective acids and double-distilled water was used throughout.

2.2 Weight loss measurements

According to the American Society for Testing and Materials (ASTM) standard procedure, the weight loss measurements were carried out. The copper specimens, in triplicate, were immersed for a period of 2 hrs at room temperature (301 ± 1 K) in 100 ml of the corrosive media both with and without the inhibitor. The average weight loss was used to calculate the inhibition efficiency using the formula:

$$IE = \left(\frac{W-W'}{W}\right) X\ 100 \qquad (1)$$

Where W and W' represent the corrosion rates in the blank and inhibited solutions respectively.

2.3 Electrochemical impedance measurements

A three electrode set up was used for electrochemical studies, in which a saturated calomel electrode (SCE) served as the reference electrode, a Pt foil served as the auxiliary electrode and the Teflon coated copper rod as the working electrode. Prior to impedance measurement, a stabilization period of 45 minutes was allowed, after immersion of the specimen in the corrosive media, which proved sufficient for E_{ocp}/Vs(SCE) to attain a stable value. Electrochemical Impedance measurements were carried out at the open circuit potential (E_{ocp}/Vs(SCE)), using a potentiostat (GAMRY REFERENCE 600) and the data were analyzed using Gamry Echem Analyst Software. The AC frequency was scanned from 100 kHz to 10 mHz, with 10 mV peak-to-peak sine wave being the excitation signal. Inhibition efficiencies (IE%) were calculated using the equation (Doner *et al.* 2011):

$$IE\% = \frac{R_{ct}^{'}-R_{ct}}{R_{ct}^{'}} X100 \qquad (2)$$

Where R_{ct} and $R_{ct}^{'}$ are the charge transfer resistance values in the blank and inhibited solutions respectively.

2.4 Polarization measurements

At a potential sweep rate of 1.6 mVs^{-1}, potentiodynamic polarization curves were recorded using the same cell setup. The potentials were scanned primarily from negative potentials through OCP to the positive side. The inhibition efficiencies were calculated employing the relationship (Shahin *et al.* 2002).

$$IE\% = \frac{i_{corr}-i_{corr}^{'}}{i_{corr}} X\ 100 \qquad (3)$$

where i_{corr} and $i_{corr}^{'}$ are the corrosion current densities in the absence and in the presence of inhibitor respectively.

2.5 Determination of Activation energy

Potentiodynamic polarization studies were carried out in the temperature range 308K to 328K in the presence and in the absence of the inhibitor in both the acid solutions in order to determine the activation energy and understand the mechanism of adsorption of the inhibitor onto copper surface. The dependence of corrosion rate on temperature is calculated using the Arrhenius equation

$$i_{corr} = A\ e^{-Ea/RT} \qquad (4)$$

Where i_{corr} is corrosion current density, R is universal gas constant, A is the Arrhenius pre-exponential constant, T is the absolute temperature and Ea is the energy of activation.

2.6 Measurement of potential of zero charge

At 20 kHz AC frequency, electrochemical impedance values were recorded at various applied DC potentials. Double layer capacitance values obtained were plotted against applied DC potentials and the PZC was obtained from the lowest point of the plot.

2.7 Study of Synergistic effect

The synergistic effect of halide ions with the inhibitor on corrosion inhibition was studied. Based on Aramki and Hackermann (1969) equation, the synergism parameter was calculated as follows

$$S_\theta = \frac{1-\theta_{1+2}}{1-\theta'_{1+2}} \quad (5)$$

Where $\theta_{1+2} = (\theta_1 + \theta_2) - (\theta_1\theta_2)$; θ_1= surface coverage by anion; θ_2 = surface coverage by cation; θ'_{1+2} = measured surface coverage by both anion and cation.

2.8 Surface morphology studies.

The surface morphologies of the corroded samples in the blank and in the presence of the inhibitor were carried out in a digital Scanning Electron Microscope. All micrographs of the specimen were taken at a magnification of 200X. These samples underwent the same pre-treatment as in electrochemical experiments before recording the SEM image.

3. RESULTS & DISCUSSION

3.1 Weight loss measurement

The inhibition efficiencies for copper in nitric acid and sulphuric acid media at different concentrations of the inhibitor are given in Table 1. As concentration of the inhibitor increases, there is sharp increase in inhibitor efficiency at initial doses, but however tend to attain a steady value with further increase (fig.1a, 1b). This is because an appreciable area of the surface gets covered already by the inhibitor through adsorption. Thus with further increase, the curve tends to flatten up, typical of a type I adsorption isotherm.

Table 1. Inhibitor efficiency from weight loss measurement for copper in 1.0M HNO_3 and 0.5M H_2SO_4 solutions at different concentrations of the inhibitor.

Medium	Inhibitor concentration (mM)	Corrosion rate (mmpy)	Inhibitor efficiency (IE%)
1.0 M HNO_3	Blank	47.2162	-
	0.0004	29.4522	37.6
	0.001	21.6986	54.0
	0.002	16.4909	65.0
	0.01	13.3084	71.8
	0.02	10.4732	77.8
0.5M H_2SO_4	Blank	22.3929	-
	0.0004	10.5889	52.7
	0.001	7.8693	64.8
	0.002	4.9184	78.0
	0.01	2.0252	90.9
	0.02	1.1572	94.8

3.2 Electrochemical impedance study

The impedance spectra recorded at room temperature in the absence and in the presence of various concentrations of the inhibitor in 1.0M nitric acid and 0.5 M sulphuric acid solutions are shown in Fig. 2a and 2b respectively.

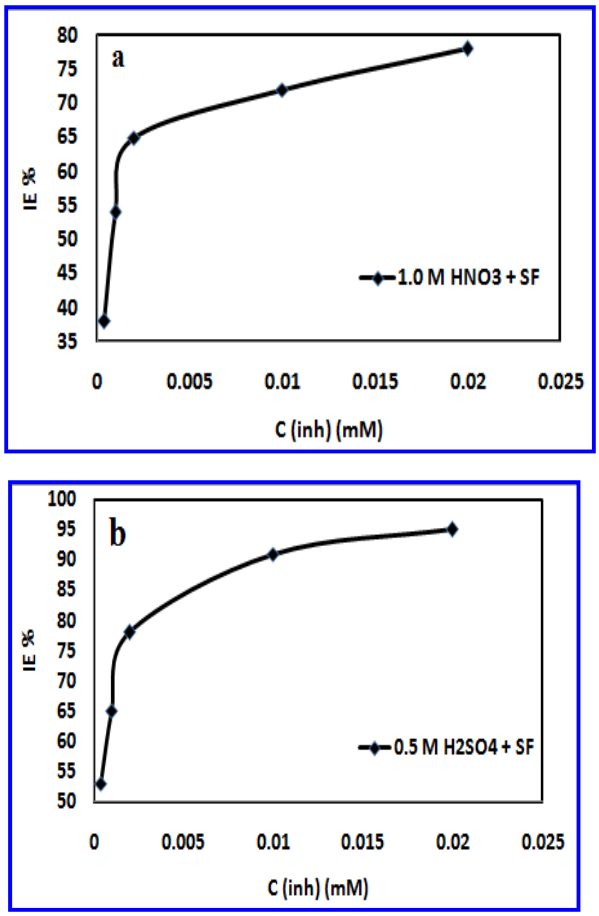

Fig. 1: Plots of inhibitor efficiency (%) with concentration of sparfloxacin in (a) HNO_3 (b) H_2SO_4

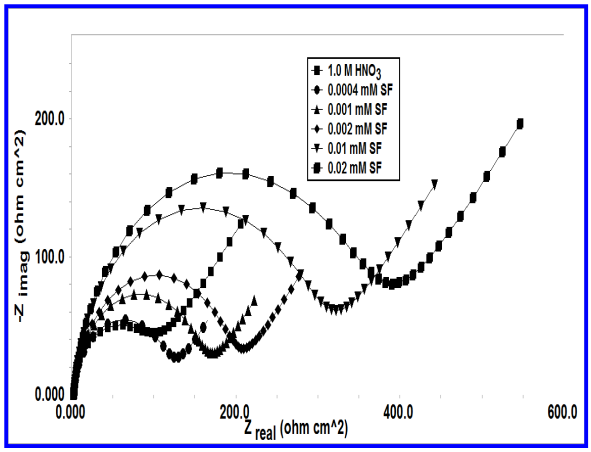

Fig. 2a: Nyquist plots for Cu electrode obtained in 1.0M HNO_3 solution at various concentrations of sparfloxacin.

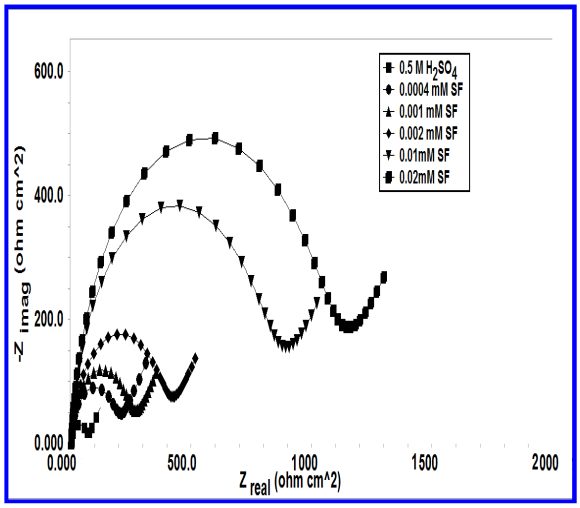

Fig. 2b: Nyquist plots for Cu electrode obtained in 0.5M H_2SO_4 solution at various concentrations of sparfloxacin

Table 2. Electrochemical parameters derived from EIS measurements for the corrosion of copper in 1.0M HNO_3 and 0.5M H_2SO_4 solutions at different concentrations of the inhibitor.

Medium	Inhibitor Concentration (mM)	Rct Ωcm^2	Y0 (X 10-6) $\Omega^{-1}cm^{-2}$	n	Cdl μFcm^{-2}	Inhibitor Efficiency IE%
HNO_3	Blank	87.0	862.0	0.99	146	-
	0.0004	112.2	682.8	0.95	122	22
	0.001	155.0	401.5	0.93	118	43
	0.002	191.0	192.7	0.92	94.1	54
	0.01	293.2	190.6	0.92	78.5	70
	0.02	356.2	180.5	0.94	63.7	75
H_2SO_4	Blank	63.0	330.0	0.93	159	-
	0.0004	183.0	261.3	0.95	128	52
	0.001	244.2	236.3	0.95	111	64
	0.002	387.0	183.7	0.94	98.2	77
	0.01	820.0	152.6	0.93	81.5	89
	0.02	1061	143.9	0.93	70.9	91

The capacitance dispersion at the solid surfaces is mainly caused by its roughness, chemical inhomogeneities, degree of polycrystallinity and anion adsorption (Rahman *et al.* 1997). Equivalent circuit given in the fig. 3 is used to analyze the impedance spectrum which displays a high frequency capacitive loop and the Warburg impedance in the low frequency (Khaled, 2010), (Ma *et al.* 2002). The appearance of the Warburg impedance is proposed to be due to the diffusion of oxygen followed by its reduction in aerated acid solutions (El Din *et al.* 2000). A constant phase element (CPE) is substituted for the capacitive element to give a more accurate fit (Wu *et al.* 1999), as the capacitive loops are depressed semi- circles rather than regular semi-circles, which has the impedance function in the following form (Rahman *et al.*1997).

$$Z_{cpe} = \frac{1}{Y_0 (j\omega)^n} \quad (6)$$

Where Y_0 is the admittance of the corrosive system at 1rad s^{-1} and n is a constant ($-1 \leq n \leq 1$). When n = 0, the CPE represents a pure resistor, if n = -1 CPE represents an inductor and if n = +1, CPE represents a pure capacitor.

The values of n for the corroding electrode in both the media are close to 1 (as it can be seen from Table 2) indicating the nearly capacitive behaviour of the CPE. The idealized capacitance value (c_{id}) is calculated from the CPE parameters using the expression (Mallaiya *et al.* 2011), (Van westing *et al.* 1993).

$$C_{id} = \frac{Y_0 \omega^{n-1}}{\sin(\frac{n\pi}{2})} \quad (7)$$

Where 'ω' is the angular frequency at the maximum value of the imaginary part of impedance -Z". It is further seen that this value of angular frequency and C_{dl} are calculated using the expression (Hsu and Mansfeld, 2001).

$$\omega_{max} = \left(\frac{1}{R_{ct} Y_0}\right)^{1/n} \quad (8)$$

$$C_{dl} = Y_0(\omega_{max})^{n-1} \quad (9)$$

Due to an increase in the surface coverage by the inhibitor, there is an increase in R_{ct} with concentration. The decrease in C_{dl} is as a result of the adsorption of the inhibitor molecule with water replacement at the metal/ solution interface which led to decrease in local dielectric constant and/or an increase in the thickness of the electrical double layer (Behpour *et al.* 2009). The gradual displacement of water molecules by the adsorption of the inhibitor onto the metal surface decreased the extent of the corrosion (Benabdellah *et al.* 2007).

3.3 Polarization measurements

The addition of inhibitor to the corrosive media changes the anodic and cathodic Tafel slopes as seen in the polarisation curves in figure 4a and 4b, indicating its influence on the respective reactions.

However, the influence was significantly more pronounced in cathodic curve and these curves are almost parallel to each other, indicating that the hydrogen evolution reaction is under activation control (Zarrouk *et al.* 2012).The inhibitor can be considered as mixed type since the maximum shift of E_{corr} in the present study is less than 85mV in both the media, (Zarrouk *et al.* 2012).

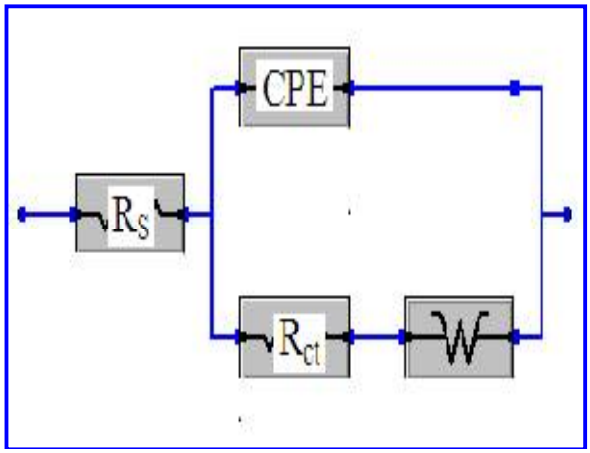

Fig. 3: Randles Equivalent Circuit

The Tafel polarization curves exhibit no steep slope in the anodic range, which indicates that no passive film is formed on the copper surface. From the Pourbaix diagram of copper, it is well known that copper is converted into Cu^{+2} and does not form its oxide film in acid media (Zarrouk *et al.* 2012). The dissolution of Cu into Cu^{+2} was not observed in deaerated acid solutions, but it dissolves in the presence of dissolved oxygen forming Cu^{+2}ion by the following mechanism

Anodic reaction:

$$Cu \rightarrow Cu^{2+} + 2e^{-} \qquad (10)$$

Cathodic reaction:

$$O_2 + 4H^{+} + 4e^{-} \rightarrow 2H_2O \qquad (11)$$

The dissolution of copper is controlled by the diffusion of soluble Cu^{+2} species from the outer Helmhotz plane to the bulk solution (Zarrouk *et al.* 2012).

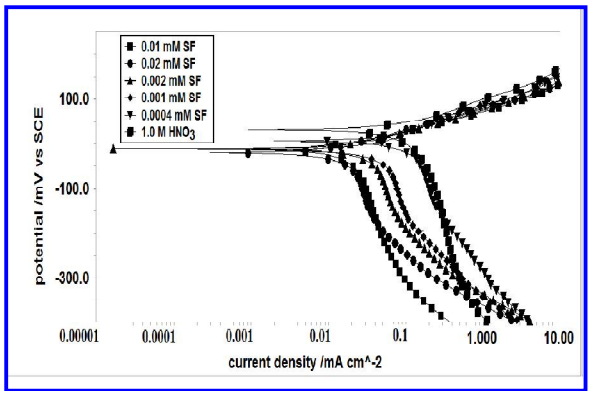

Fig. 4a: Tafel plots for Cu in 1.0M HNO_3 solution at various concentrations of sparfloxacin

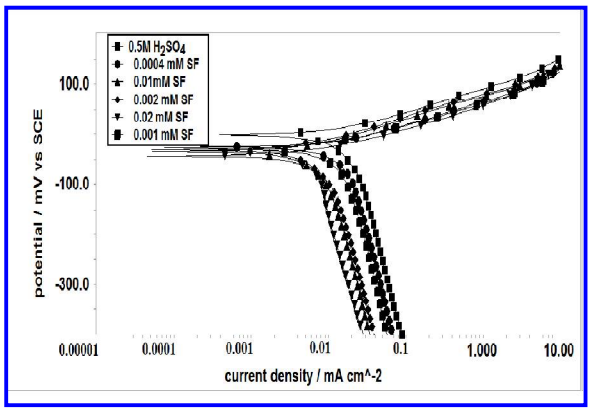

Fig. 4b: Tafel plots for Cu in0.5M H_2SO_4 solution at various concentrations of sparfloxacin

Table 3. Electrochemical parameters for the corrosion of copper in 1M HNO_3 and 0.5M H_2SO_4 solutions at different concentrations of the inhibitor derived from Tafel polarization curves

Medium	Concentration (mM)	E_{corr}(mV)	i_{corr}(µA cm^-2)	βc (mV)	βa (mV)	Corrosion rate(mpy)	IE%
HNO_3	Blank	42.10	109	363.1	66.0	175.7	-
	0.0004	7.22	80.5	204.0	69.8	129.9	26
	0.001	-14.40	42.8	161.5	67.3	68.98	61
	0.002	-11.70	38.0	147.7	53.1	61.85	65
	0.01	-12.3	27.0	265.6	47.2	43.56	75
	0.02	-20.30	25.1	136.6	50.7	41.04	77
H_2SO_4	Blank	4.52	23.0	301.9	49.10	37.20	-
	0.0004	-26.80	17.0	374.6	49.30	28.13	26
	0.001	-29.80	11.3	382.9	47.70	18.37	51
	0.002	-43.20	6.60	601.3	44.50	10.68	71
	0.01	-35.20	5.18	242.2	49.60	8.37	77
	0.02	-31.50	4.15	212.9	48.80	7.84	82

The electrochemical parameters such as corrosion potential (E_{corr}), corrosion current (i_{corr}), cathodic and anodic Tafel slopes, and inhibitor efficiencies are listed in Table 3. The higher βc on comparison with βa in the table 3 shows a higher influence on the retardation of cathode reduction rate than anodic metal dissolution, though βc and βa change with increase in inhibitor concentration (Sanghvi *et al.* 1999). This indicated that sparfloxacin retards the cathodic reaction to a larger extent than the anodic dissolution. It shows higher inhibition efficiency for the dissolution of copper in sulphuric acid solution than in nitric acid solution.

3.4 Adsorption isotherm

The adsorption of sparfloxacin molecules at the metal solution interface can be considered as a substitution process where an organic compound (org_{sol}) from the aqueous medium displaces the water molecules associated with the metal surface (H_2O_{ads}).

$$Org_{(sol)} + xH_2O_{ads} \rightarrow Org_{ads} + xH_2O \qquad (12)$$

Where 'x' is the number of water molecules replaced by the adsorption of one sparfloxacin molecule. Using the R_{ct} values, the surface coverage (θ) of the inhibitor was calculated using the relation,

$$\theta = \frac{R'_{ct} - R_{ct}}{R'_{ct}} \qquad (13)$$

Where R'_{ct} and R_{ct} are the charge transfer resistance values in the inhibited and blank solutions respectively. Analysis showed that the adsorption followed Langmuir isotherm, given by the expression (Mallaiya *et al.* 2011), (Zarrouk *et al.* 2012), (Joseph and Joseph, 2011).

$$C_{inh}/\theta = C_{inh} + 1/K_{ads} \qquad (14)$$

Where C_{inh} is the concentration of the inhibitor, θ is the surface coverage and K_{ads} is the adsorption equilibrium constant. At constant temperature, the value of K_{ads} is determined from the plot of C_{inh} vs C_{inh}/θ.

The standard free energy of adsorption is calculated using the expression:

$$K_{ads} = 1/55.5 \exp^{-\Delta G/RT} \qquad (15)$$

Where T is the thermodynamic temperature, R is the universal gas constant, ΔG is the free energy of adsorption and 55.5 is the concentration of water in the solution in mol L-1.

Langmuir Adsorption Isotherm for the adsorption of sparfloxacin on the copper metal surface in 1.0M HNO_3 and in 0.5M H_2SO_4 solutions are given in fig 5. The plots obtained were linear with correlation coefficients greater than 0.9.The calculated values of ΔG_{ads} at room temperature in nitric acid and sulphuric acid solutions are -45.96kJmol^{-1} and -45.46kJmol^{-1} respectively. The negative values of ΔG_{ads} indicate the spontaneous adsorption of sparfloxacin molecules onto the metal surface. In the present study, the values of -ΔG_{ads} are greater than 40 kJmol-1 which indicate that the sparfloxacin molecules get adsorbed onto the metal surface by chemisorption (Bentiss *et al.* 1999).

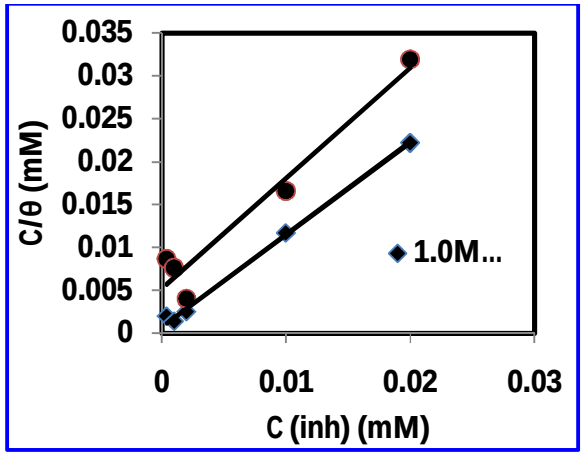

Fig. 5: Langmuir Adsorption Isotherm for the adsorption of sparfloxacin on the copper metal surface in 1.0M HNO_3 and in 0.5M H_2SO_4 solutions.

3.5 Effect of temperature

The various electrochemical parameters obtained at different temperatures, are given in Table 4.Inspection of the table shows that the inhibitor efficiency and corrosion rate increases with increase in temperature. The increase in inhibitor efficiency indicates that the surface area covered by the inhibitor molecule increases which decreases the rate of dissolution.

The Arrhenius plots and Transition state plots are shown in Figures 6 and 7.Inspection of Table 5 shows that the values of E_a determined in the presence of sparfloxacin are lower than that in the blank solution. This is an indication of decrease in energy barrier for the adsorption of the inhibitor molecules on copper surface. The surface area covered by the inhibitor molecule increases with increase in temperature and the metal dissolution rate in the corrosive media is controlled by diffusion of the corrosion product through the protective film of the inhibitor molecule (Szauer and Brandt, 1981). The

decrease in E_a with the addition of inhibitor in both the media reveals that the inhibitor molecules are adsorbed onto the metal surface by chemisorptions (Szauer and Brandt, 1981), (Ivanov, 1986), (Ma *et al.* 2003), (Solmaz *et al.* 2008). The negative entropy value indicates that activated state has more association and has less disorder. The negative value of ΔH implies that the adsorption is an exothermic process.

Table 3 Electrochemical parameters from Tafel polarization curves for the corrosion of copper in 1.0M HNO_3 and 0.5 M H_2SO_4 solutions at different temperatures.

Medium	Concentration (mM)	Temperature (K)	E_{corr} (mV)	i_{corr} µA / cm^2	B_c (mV)	β_a (mV)	Corrosion rate (mpy)	IE %
HNO_3	Blank	308	2.59	30.3	173.6	54.40	49.04	-
	Blank	318	10.80	199.0	411.4	65.70	322.6	-
	Blank	328	21.70	358.0	440.0	59.90	579.2	-
	0.02mM	308	6.420	14.8	373.6	77.7	23.90	51
	0.02mM	318	8.890	72.8	330.3	61.0	117.8	63
	0.02mM	328	14.10	94.8	415.3	63.0	153.5	74
H_2SO_4	Blank	308	-14.00	12.2	537.3	49.10	19.82	-
	Blank	318	-46.67	30.4	281.0	50.23	49.19	-
	Blank	328	11.70	88.5	271.9	62.89	143.2	-
	0.02mM	308	-54.9	7.030	104.8	45.30	14.65	42
	0.02mM	318	-31.8	12.60	219.2	46.0	20.45	59
	0.02mM	328	-39.9	16.44	193.2	46.4	26.59	81

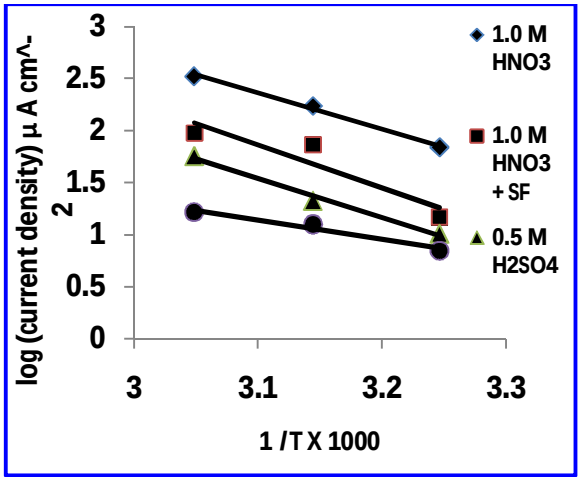

Fig. 6: Typical Arrhenius plots for corrosion of Cu in 1.0 M HNO_3 and in 0.5M H_2SO_4 solution.

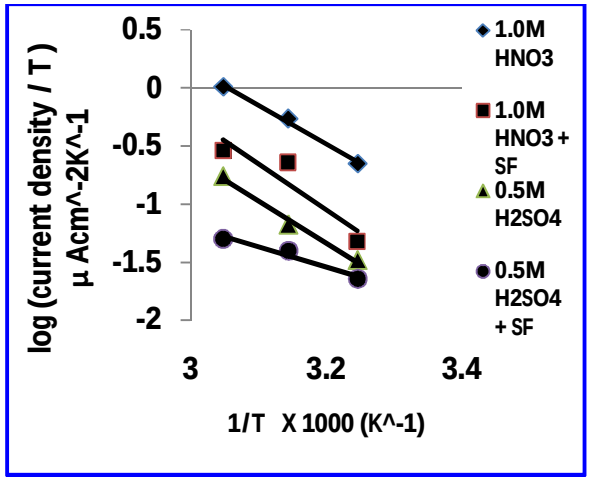

Fig. 7: Transition state plots for corrosion of Cu in 1.0M HNO_3 and in 0.5 M H_2SO_4 solution.

Table 4. Thermodynamic parameters obtained from potentiodynamic polarization studies.

Medium	Inhibitor concentration (mM)	Kads (M-1)	ΔGads kJ/mole	ΔH kJ /mole	ΔS (J/mole/K)	Ea (kJ / mole)	R
HNO_3	Blank	-	-	-63.7	-26.8	66.44	0.993
	0.02	1807174	-45.96	-56.7	-70.2	59.39	0.866
H_2SO_4	Blank	-	-	-69.5	-38.2	72.19	0.989
	0.02	1478764	-45.46	-33.1	-120.7	35.80	0.858

The negative value of ΔH implies that the adsorption is an exothermic process. The negative entropy change value indicates that the activated state has more association and has less disorder. Before the adsorption of inhibitor onto the metal surface, the inhibitor molecule might freely move in the bulk solution, but with the progress in adsorption, inhibitor molecules are adsorbed in orderly manner onto the metal surface causing entropy to decrease (Szauer & Brand, 1981).

3.6 Potential of zero charge

The surface charge of the metal is determined from the open circuit potential with respect to the PZC (Ramesh Saliyan and Adhikari, 2008). The dependency of the double layer capacitance on the applied DC potential in the absence and in the presence of sparfloxacin in nitric acid and sulphuric acid are shown in the fig. 8 and 9. The Eocp and PZC data are given in the table 6.

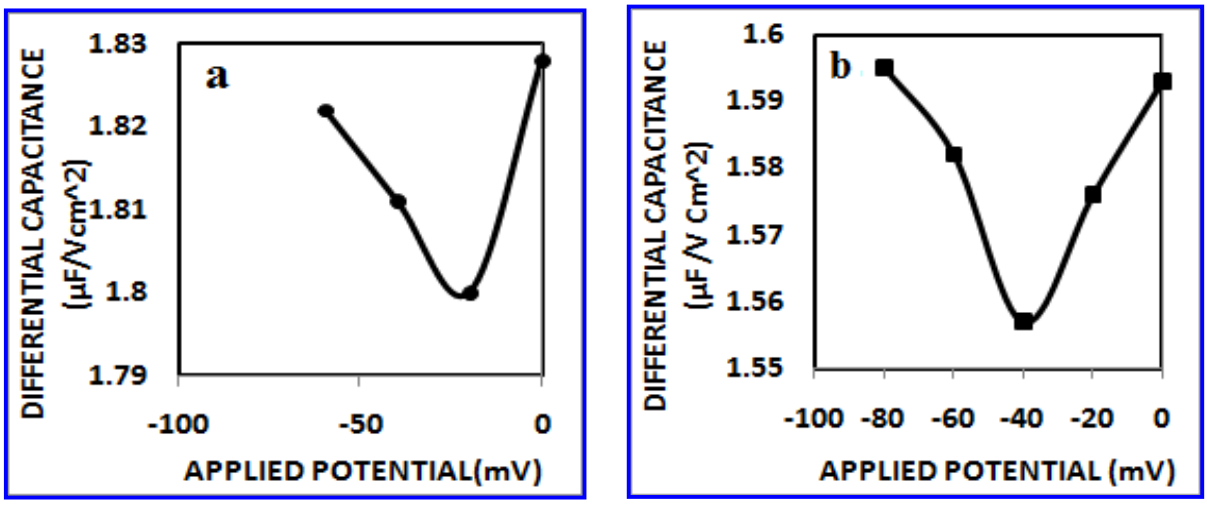

Fig. 9: Plot of differential capacitance vs applied potential for copper in (a) 0.5M H_2SO_4 (b) 0.5M H_2SO_4 containing 0.01mM sparfloxacin.

Table Error! No text of specified style in document.. Excess charge on Cu electrode in 1.0M HNO_3 and 0.5M H_2SO_4 solutions in the presence and absence of the inhibitor

Medium	E_{OCP} (mV/SCE)	E_{PZC} (mV/SCE)	Excess charge E_{OCP} - E_{PZC}(mV)
1.0M HNO_3	+42.10	+40	+2.1
1.0MHNO_3+0.01mM of inhibitor	-12.3	-20	+7.7
0.5M H_2SO_4	+4.52	-20	+24.52
0.5MH_2SO_4+0.01mMof inhibitor	-35.2	-40	+4.8

As seen from the table 6, the metal surface is positively charged with respect to PZC, based on which the mechanism proposed is that the sulphate and nitrate ions will first get adsorbed onto the metal surface, (Ramesh Saliyan and Adhikari, 2008), (Popova, 2003), (Solmaz *et al.* 2008), and the protonated inhibitor molecules make bond with the anions and prevent the metal dissolution (Doner *et al.* 2011).

3.7 Synergistic effect of halide ions

When two or more corrosion inhibitors are added to a corrosive environment of a metal, the inhibitor efficiency of the mixture may be greater than the sum of each one of the additives due to synergy.

The surface charge of copper at the OCP was found to be positive in the presence of halide ions in sulphuric acid and nitric acid solutions and hence the mechanism proposed is that the halide ions(X^-) will first get adsorbed onto the metal surface, (Ramesh Saliyan and Adhikari, 2008), (Popova, 2003), (Solmaz *et al.* 2008) and the protonated inhibitor molecules (HI^+) make bond with the anions and prevent the metal dissolution (Doner *et al.* 2011) and is given in the equations 16 and 17.

Table 7. Electrochemical parameters for copper in 1M HNO_3 and 0.5M H_2SO_4 solutions in the presence of KCl, KBr and KI from EIS.

Medium	Inhibitor Concentration (mM)	Y0 (X 10-6) Ω-1cm-2	n	Rct Ωcm2	θ	S_θ
1.0M HNO_3	Blank	862.9	0.997	87	-	-
	0.002mM SF	192.7	0.922	191	0.5445	-
	0.5mM KCl	189.1	0.898	313	0.7220	-
	0.002mM SF+ 0.5mM KCl	53.50	0.973	495.9	0.8245	0.7213
	0.5mM KBr	271.0	0.912	231.8	0.6246	-
	0.002mM SF+ 0.5mM KBr	140.2	0.967	456	0.8092	0.8957
	0.5mM KI	99.5	0.905	123	0.2926	-
	0.002mM SF+ 0.5mM KI	110.2	0.925	948.7	0.9082	3.50
0.5M H_2SO_4	Blank	330	0.930	63	-	-
	0.002mM SF	203.7	0.921	387	0.7751	-
	0.5mM KCl	349.1	0.945	191	0.6701	-
	0.002mM SF+ 0.5mM KCl	359.2	0.945	248.6	0.7465	0.2923
	0.5mM KBr	256.7	0.934	154	0.5909	-
	0.002mM SF+ 0.5mM KBr	153.2	0.963	606	0.8960	0.8846
	0.5mM KI	152.6	0.926	174	0.6379	-
	0.002mM SF+ 0.5mM KI	70.3	0.939	2228	0.9717	2.87

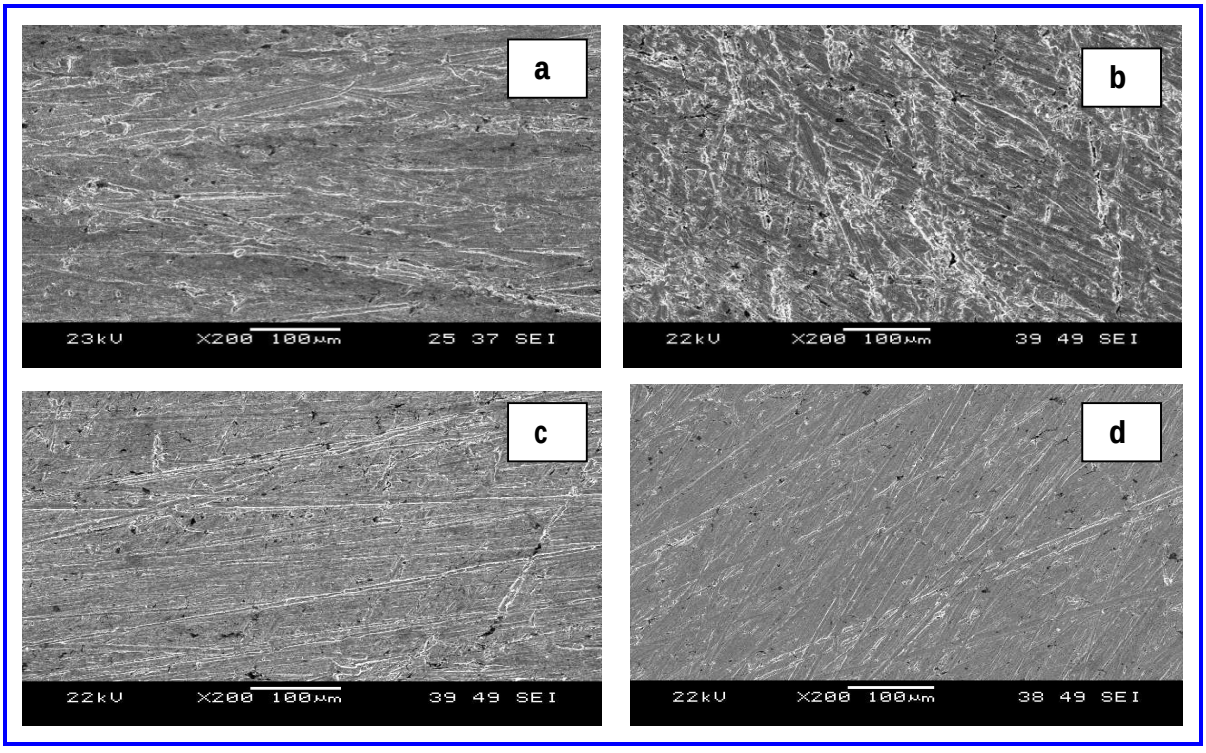

Fig. 10: SEM micrograph of copper specimen after immersion in a) 1.0M HNO_3. b) 0.5M H_2SO_4. c)1.0M HNO_3 containing sparfloxacin. d) 0.5M H_2SO_4 containing sparfloxacin

$$X^{-}{}_{S} \quad \_ \quad X^{-}{}_{ads} \qquad (16)$$

$$X^{-}{}_{ads} + HI^{+}{}_{S} \quad \_ \quad (X^{-}\text{-}HI^{+})_{ads} \qquad (17)$$

Thus the halide ions are able to improve adsorption of the organic cations by forming intermediate bridges between the positively charged metal surface and the positive end of the organic inhibitor and results in increased surface coverage (Özcan *et al.* 2008),(Zhao and chen, 2012), (Feng *et al.* 1999), (Obot *et al.* 2009), (Umoren *et al.* 2010), (Umoren *et al.* 2008), (Pavithra, *et al.* 2010), (Ai *et al.* 2006). The synergism parameters S_{θ} calculated using the impedance studies with the addition of potassium chloride, potassium bromide and potassium iodide are shown in the Table 7. In the present case the addition of iodide ions give S_{θ} value as 3.50 and 2.87 in nitric acid and sulphuric acid media respectively and shows synergistic effect in both the acid media. The greater influence of the iodide ion is often attributed to its large ionic radius, high hydrophobicity and low electronegativity (Bentiss *et al.* 2002) which helps in the adsorption of the inhibitor molecules onto the metal surface (Ramesh Saliyan and Adhikari, 2008).

3.8 Surface morphology

The SEM micrographs of copper specimen exposed to the acid solutions are shown in Fig. 10a and 10b. These pictures clearly depict the high density pits due to the exposure of copper in acid media. The influences of the addition of 0.01mM sparfloxacin to the corrosive media are shown in Fig. 10c and 10d. It shows the formation of protective film on the surface of copper specimen in the presence of sparfloxacin. The micrographs show no evidence of pitting, which is attributed to the protection provided by the adsorption of inhibitor molecules onto the metal surface.

4. CONCLUSION

(i) In both nitric acid and sulphuric acid media, the inhibitor efficiency increases with increase in sparfloxacin concentration and about 90% efficiency was observed at 0.02 mM dose. The obtained results show that sparfloxacin can act as a good inhibitor for the corrosion of copper in both the acid media.

(ii) The potentiodynamic polarization curves indicated that this molecule acts as a mixed type of inhibitor.

(iii) The adsorption of sparfloxacin onto metal surface follows Langmuir adsorption isotherm.

(iv) The value of free energy of adsorption greater than -40kJmol-1 indicates that the adsorption is through chemisorption. The decrease in Ea with the addition of inhibitor also supports this fact.

(v) Determination of PZC indicates the formation of sulphate and nitrate inter connecting bridges in the adsorption of the inhibitor onto the metal surface in both the acid media.

(vi) The negative sign of ΔH_{ads} indicates that the adsorption of inhibitor molecule is an exothermic process. The negative value of ΔS_{ads} in the presence of the inhibitor reveals that activated state has more association and has less disorder.

ACKNOWLEDGEMENT

The authors gratefully acknowledge the facilities provided by the Principal and the Management of Coimbatore Institute of Technology and PSG College of Technology, Coimbatore.

REFERENCES

Ai, J., Guo, X., Qu, J., Chen, Z. and Zheng, J., Adsorption behavior and synergistic mechanism of a cationic inhibitor and KI on the galvanic electrode, *Colloids and Surfaces A: Physicochemical and Engineering Aspects*, 281(1), 147-155(2006). doi:10.1016/j.colsurfa.2006.02.031

Aramaki, K. and Hackerman, N., Inhibition mechanism of medium-sized polymethyleneimine, *J. Electrochem. Soc.*, 116(5), 568-574(1969). doi: 10.1149/1.2411965

Behpour, M., Ghoreishi, S., Gandomi-Niasar, A., Soltani, N. and Salavati-Niasari, M., The inhibition of mild steel corrosion in hydrochloric acid media by two Schiff base compounds, *J. Mater. Sci.*, 44(10), 2444-2453(2009). doi:10.1007/s10853-009-3309-y

Benabdellah, M., Touzani, R., Aouniti, A., Dafali, A., El Kadiri, S., Hammouti, B. and Benkaddour, M., Inhibitive action of some bipyrazolic compounds on the corrosion of steel in 1M HCl: Part I: Electrochemical study, *Mater. Chem. Phys.*, 105(2), 373-379(2007). doi:10.1016/j.matchemphys.2007.05.001

Bentiss, F., Bouanis, M., Mernari, B., Traisnel, M. and Lagrenee, M., Effect of iodide ions on corrosion inhibition of mild steel by 3, 5-bis (4-methylthiophenyl)-4H-1, 2, 4-triazole in sulfuric acid solution', *J. Appl. Electrochem.*, 32(6), 671-678(2002). doi:10.1023/A:1020161332235

Bentiss, F., Traisnel, M., Gengembre, L. and Lagrenée, M., A new triazole derivative as inhibitor of the acid corrosion of mild steel: electrochemical studies, weight loss determination, SEM and XPS', *Applied surface science*, 152(3), 237-249(1999). doi:10.1016/S0169-4332(99)00322-0

Döner, A., Solmaz, R., Özcan, M. and Kardaş, G., Experimental and theoretical studies of thiazoles as corrosion inhibitors for mild steel in sulphuric acid solution', *Corros. Sci.*, 53(9), 2902-2913(2011). doi:10.1016/j.corsci.2011.05.027

El Din, A. S., El Dahshan, M. and El Din, A. T., Dissolution of copper and copper-nickel alloys in aerated dilute HCl solutions, *Desalination*, 130(1), 89-97(2000). doi: 10.1016/s0011-9164(00)00077-1

Feng, Y., Siow, K., Teo, W. and Hsieh, A., The synergistic effects of propargyl alcohol and potassium iodide on the inhibition of mild steel in 0.5 M sulfuric acid solution, *Corros. Sci.*, 41(5), 829-852(1999). doi:10.1016/S0010-938X(98)00144-9

Hsu, C. and Mansfeld, F., Technical note: concerning the conversion of the constant phase element parameter Y_0 into a capacitance, *Corros. Sci.*, 57(9), 747-748(2001). doi:10.5006/1.3280607

Ivanov, E., Inhibitors for metal corrosion in acid media, Metallurgy, Moscow(1986).

Joseph, B. and Joseph, A., Inhibition of Copper Corrosion in 1 M Nitric Acid-Electro Analytical and Theoretical Study with (E)-(4-(4-Methoxybenzylideneamino)-4H-1, 2, 4-Triazole-3, 5diyl) Dimethanol (MBATD), *Portugaliae Electrochimica. Acta*., 29(4), 253-271(2011). doi:10.4152/pea.201104253

Khaled, K., Corrosion control of copper in nitric acid solutions using some amino acids–A combined experimental and theoretical study, *Corros. Sci.*, 52(10), 3225-3234(2010). doi:10.1016/j.corsci.2010.05.039

Ma, H., Chen, S., Niu, L., Zhao, S., Li, S. and Li, D., Inhibition of copper corrosion by several Schiff bases in aerated halide solutions, *J. Appl. Electrochemi.*, 32(1), 65-72(2002). doi:10.1023/A:1014242112512

Ma, H., Chen, S., Yin, B., Zhao, S. and Liu, X., Impedance spectroscopic study of corrosion inhibition of copper by surfactants in the acidic solutions, *Corros. Sci.*, 45(5), 867-882(2003). doi:10.1016/S0010-938X(02)00175-0

Mallaiya, K., Subramaniam, R., Srikandan, S. S., Gowri, S., Rajasekaran, N and Selvaraj, A., Electrochemical characterization of the protective film formed by the unsymmetrical Schiff's base on the mild steel surface in acid media, *Elect. Acta*, 56(11), 3857-3863(2011). doi:10.1016/j.electacta.2011.02.036

Obot, I., Obi-Egbedi, N. and Umoren, S., The synergistic inhibitive effect and some quantum chemical parameters of 2,3-diaminonaphthalene and iodide ions on the hydrochloric acid corrosion of aluminium, *Corros. Sci.*, 51(2), 276-282(2009). doi:10.1016/j.corsci.2008.11.013

Özcan, M., Solmaz, R., Kardaş, G. and Dehri, I., Adsorption properties of barbiturates as green corrosion inhibitors on mild steel in phosphoric acid, *Colloids and Surfaces A: Physicochemical and Engineering Aspects*, 25(1-2), 57-63(2008). doi:10.1016/j.colsurfa.2008.04.031

Pavithra, M., Venkatesha, T., Vathsala, K. and Nayana, K., Synergistic effect of halide ions on improving corrosion inhibition behaviour of benzisothiozole-3-piperizine hydrochloride on mild steel in 0.5 M H_2SO_4 medium, *Corros. Sci.*, 52(11), 3811-3819(2010). doi:10.1016/j.corsci.2010.07.034

Popova, A., Sokolova, E., Raicheva, S. and Christov, M., AC and DC study of the temperature effect on mild steel corrosion in acid media in the presence of benzimidazole derivatives, *Corros. Sci.*, 45(1), 33-58(2003).

Rahman, K. M., Schneider, S. C. and Seitz, M. A., Hopping and Ionic Conduction in Tin Oxide-Based Thick-Film Resistor Compositions, *J. Am. Ceram. Soc.*, 80(5), 1198-1202(1997). doi:10.1111/j.1151-2916.1997.tb02964.x

Şahin, M., Bilgic, S. and Yılmaz, H., The inhibition effects of some cyclic nitrogen compounds on the corrosion of the steel in NaCl mediums, *Appl. Surf. Sci.*, 195(1), 1-7(2002). doi:10.1016/S0169-4332(01)00783-8

Saliyan, V. R. and Adhikari, A. V., Quinolin-5-ylmethylene-3-{[8-(trifluoromethyl) quinolin-4-yl] thio} propanohydrazide as an effective inhibitor of mild steel corrosion in HCl solution, *Corros. Sci.*, 50(1), 55-61(2008). doi.10.1016/j.corsci.2006.06.035

Sanghvi, M., Shukla, S., Misra, A., Padh, M. and Mehta, G., Inhibition of hydrochloric acid corrosion of mild steel by aid extracts of embilica officianalis, terminalia bellirica and terminalia chebula, *Bulletin of Electrochemistry*, 13(8-9), 358-361(1997).

Solmaz, R., Kardaş, G., Culha, M., Yazıcı, B. and Erbil, M., Investigation of adsorption and inhibitive effect of 2-mercaptothiazoline on corrosion of mild steel in hydrochloric acid media, *Electrochimica Acta*, 53(20), 5941-5952(2008). doi.10.1016/j.electacta.2008.03.055

Szauer, T. and Brandt, A., Adsorption of oleates of various amines on iron in acidic solution, *Electrochimica Acta*, 26(9), 1253-1256(1981). doi:10.1016/0013-4686(81)85107-9

Umoren, S., Li, Y. and Wang, F., Synergistic effect of iodide ion and polyacrylic acid on corrosion inhibition of iron in H_2SO_4 investigated by electrochemical techniques, *Corros. Sci.*, 52(7), 2422-2429(2010). doi:10.1016/j.corsci.2010.03.021

Umoren, S., Ogbobe, O., Igwe, I. and Ebenso, E., Inhibition of mild steel corrosion in acidic medium using synthetic and naturally occurring polymers and synergistic halide additives, *Corros. Sci.*, 50(7), 1998-2006(2008). doi:10.1016/j.corsci.2008.04.015

Van Westing, E., Ferrari, G. and De Wit, J., The determination of coating performance with impedance measurements-I. Coating polymer properties, *Corros. Sci.*, 34(9), 1511-1530(1993). doi: 10.1016/0010-938x(93)90245-c

Wu, X., Ma, H., Chen, S., Xu, Z. and Sui, A., General equivalent circuits for faradaic electrode processes under electrochemical reaction control, *J. Electrochem. Soc.*, 146(5), 1847-1853(1999). doi:10.1149/1.1391854

Zarrouk, Hammouti, B., Zarrok, H., Bouachrine, M., Khaled, K. and Al-Deyab, S., Corrosion inhibition of copper in nitric acid solutions using a new triazole derivative, *Int. J. Electrochem. Sci.*, 7(1), 89-105(2012).

Zhao, J. and Chen, G., The synergistic inhibition effect of oleic-based imidazoline and sodium benzoate on mild steel corrosion in a CO_2-saturated brine solution, *Electrochimica Acta*, 69, 247-255(2012). doi:10.1016/j.electacta.2012.02.101